Structurally Homologous Ligand Binding of Integrin Mac-1 and Viral Glycoprotein C Receptors

DARIO C. ALTIERI,* ORLI R. ETINGIN, DARYL S. FAIR, TERENCE K. BRUNCK, JOHN E. GELTOSKY, DAVID P. HAJJAR, THOMAS S. EDGINGTON

Three spatially distant surface loops were found to mediate the interaction of the coagulation protein factor X with the leukocyte integrin Mac-1. This interacting region, which by computational modeling defines a three-dimensional macromotif in the catalytic domain, was also recognized by glycoprotein C (gC), a factor X receptor expressed on herpes simplex virus (HSV)–infected endothelial cells. Peptidyl mimicry of each loop inhibited factor X binding to Mac-1 and gC, blocked monocyte generation of thrombin, and prevented monocyte adhesion to HSV-infected endothelium. These data link the ligand recognition of Mac-1 to established mechanisms of receptor-mediated vascular injury.

INITIATION OF COAGULATION ON VASCULAR cells is implicated in various immune and inflammatory reactions and contributes to vascular injury and atherogenesis (*1*). Leukocytes, platelets, and endothelial cells each interact with coagulation proteins through regulated, receptor-mediated assembly (*2*). On stimulated monocytes, the Mac-1 receptor (CD11b/CD18), a leukocyte-restricted member of the integrin gene superfamily (*3*), binds with high affinity the coagulation serine zymogen factor X (*4*). Similarly, upon HSV infection, endothelial cells express the viral gC receptor, which also binds factor X avidly (*5*). On both cell types, the bound factor X is converted to the protease factor Xa by limited proteolytic activation, leading to the local generation of thrombin with its pleiotropic effects such as increased monocyte adhesion to virally infected endothelium (*4, 5*).

To identify the structurally interactive sites on factor X that are recognized by vascular cell receptors, we have generated a panel of partially overlapping synthetic peptides representative of selected regions of the factor X molecule (Table 1). Each peptide was initially tested in a quantitative receptor-ligand binding assay for its ability to competitively inhibit the binding of ^{125}I-labeled factor X to monocytic THP-1 cells that had been stimulated with the chemoattractant NH_2-formyl-Met-Leu-Phe (N-fMLP). Three peptides from noncontiguous linear sequences in the catalytic domain of factor X, representing predicted surface loops, inhibited ^{125}I–factor X binding to monocyte Mac-1 (Table 1) and were further characterized. Reanalysis of variant peptides synthesized with various amino acid permutations identified a minimal inhibitory core sequence for each of the three implicated regions. The factor X peptides GYDTKQEDG (366 to 373), IDRSMKTRG (422 to 430), and GLYQAKRFKVG (238 to 246), each inhibited ^{125}I–factor X binding to monocyte Mac-1 in a concentration-dependent fashion [concentration that inhibits binding by 50% (IC_{50}) = 1 to 5 μM] (Fig. 1A) (*6*). In parallel experiments, sequence-specific antibodies that were generated to each of these three peptides blocked ^{125}I–factor X binding to monocytes in a concentration-dependent manner (*7*), thus providing independent and convergent evidence for the specificity of recognition.

Using an in vitro model of arterial injury that may mimic one of the earliest described pathogenic events in some forms of atherosclerosis (*5*), we observed that the same three peptidyl ligands also inhibited ^{125}I–factor X binding in a concentration-dependent fashion (IC_{50} = 60 to 80 μM) to the HSV protein gC of viral-infected endothelium (Fig. 1B). Control peptides in which the sequence was scrambled did not diminish ^{125}I–factor X binding to monocytes or HSV-infected endothelium. As in previous studies, binding and activation of factor X by Mac-1 and gC culminated in local generation of thrombin and increased monocyte adhesion to HSV-infected endothelium (*4, 5*). Each of the three peptides prevented these downstream effects by blocking factor Xa-mediated monocyte procoagulant activity and suppressed monocyte adhesion to HSV-infected endothelium to that observed for noninfected cells (Table 2). Consistent with their postulated interaction with Mac-1 and gC rather than with factor X, none of the three inhibitory peptides affected the proteolytic activity of the active enzyme, factor Xa (*8*).

The three functional recognition sites in factor X were topographically mapped by computational modeling based on crystallographic data for the homologous zymogen trypsinogen. The energy-minimized structure of the catalytic domain of factor X indicated that the three peptidyl loci do not cluster in a spatially contiguous region in the molecule to form a single structure. Rather, they are found in three distant surface loops that "surround" an unobstructed catalytic active site (Fig. 2). This structural organization is consistent with a three dimensional macromotif of coordinated tripartite ligand recognition on this protein (Fig. 2).

Three major conclusions can be drawn from this study. First, ligand binding of

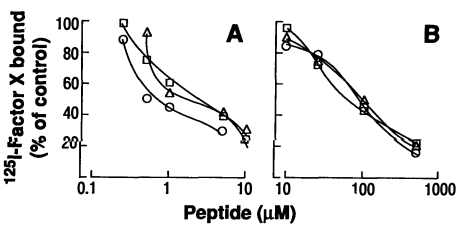

Fig. 1. Effects of factor X synthetic peptides on ^{125}I–factor X binding to monocyte THP-1 (**A**) or HSV-infected endothelial cells (**B**). The experimental conditions for ^{125}I–factor X binding to monocyte THP-1 cells are the same as in (*16*). ^{125}I–factor X binding to HSV-infected endothelial cells was quantitated as described in (*5*). Increasing concentrations of the three factor X peptides that had a minimal inhibitory core sequence were separately mixed with 10 μM fMLP-stimulated THP-1 cells (A) or HSV-infected endothelial cells (B) and 15 nM ^{125}I–factor X. At equilibrium, specific binding was calculated as described in (*16*). Peptide 1 sequence: GYDTKQED(G) (366 to 373) (○); peptide 2 sequence: IDRSMKTRG (422–430) (□); peptide 3 sequence: (G)LYQAKRFKV(G) (238 to 246) (△). In parentheses, residues added to natural sequence. In peptide 3, G in position 237 substitutes natural C. Lineweaver-Burke analysis of binding isotherms revealed that only peptide 2 (IDRSMKTRG, 422 to 430) inhibited in a characteristic competitive fashion the binding of factor X (Control, measure of fit of line (r) = 0.99, y' = 4.32; peptide 2, r = 0.99, y' = 4.8), whereas the other two peptides produced noncompetitive inhibition profiles (peptide 1, r = 0.97, y' = 21.7; peptide 3, r = 0.99, y' = 18). The data suggest that, rather than requiring the three sequences simultaneously, proper ligand alignment may be facilitated by a preferred sequential order of addition, where the noncompetitive ligand loops participate in secondary interactions and cooperatively stabilize receptor-ligand docking. Under comparable experimental conditions, scrambled control peptides synthesized for each inhibitory sequence did not affect ^{125}I–factor X interaction with either cell type.

D. C. Altieri and T. S. Edgington, Department of Immunology, Scripps Research Institute, La Jolla, CA 92037.
O. R. Etingin and D. P. Hajjar, Departments of Biochemistry and Pathology, Cornell University Medical College, New York, NY 10021.
D. S. Fair, Department of Biochemistry, University of Texas Health Center, Tyler, TX 75710.
T. K. Brunck, Corvas International Inc., 3030 Science Park Road, San Diego, CA 92121.
J. E. Geltosky, R. W. Johnson Pharmaceutical Research Institute, 3535 General Atomics Court, San Diego, CA 92121.

*To whom correspondence should be addressed.

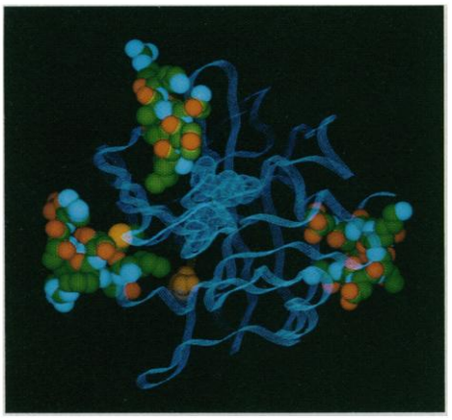

Fig. 2. Structural model of factor X catalytic domain. Homology model-building techniques (*18*) were used to construct a model of the catalytic domain of factor X from a crystal structure of trypsinogen (*19*). Structurally conserved regions were identified by visual inspection of the structures of trypsin, chymotrypsin, elastase, and kallikrein (*20*), and the factor X sequence was aligned manually with the sequences of these proteases. Atomic coordinates for backbone and conserved side chains of factor X were assigned directly from trypsinogen for the structurally conserved regions. Coordinates of nonconserved side chains within structurally conserved regions were computed for minimal overlap with other atoms. Atomic coordinates for structurally variable (loop) regions were taken from a prior model of factor Xa (*21*). The initial model structure was energy minimized in stages, first allowing all side chains to relax, and then relaxing all side chains with the backbone atoms of the loop regions. Backbone of factor X catalytic domain, ribbon diagram. Catalytic triad indicated as a blue van der Waals surface (center); loop peptide 1 (GYDTKQED), CPK model surface (right); loop peptide 2 (IDRSMKTRG), CPK surface (left); loop peptide 3 (LYQAKRFKV), CPK surface (top); Cys residue disulfide bridge between heavy and light chain, yellow CPK (lower center). The NH_2-terminus of the heavy chain is located just above peptide 1, the substrate binding groove is approximately vertical and to the right of the catalytic triad (blue van der Waals); the COOH-terminus of the model (lacking 18 residues of factor X sequence for which no structural information is available) is the COOH-terminus of peptide 2.

disparate integrins depends on the recognition of multiple and independent sites in the ligand protein. By analogy with the platelet integrin $\alpha_{IIb}\beta_3$ that can recognize different and spatially distant sites in fibrinogen (*9*), Mac-1 recognition of factor X is mediated by three spatially distant and nonhomologous surface loops. Second, the zymogen of the coagulation protease cascade factor X contains a proposed "vascular cell binding domain" that binds to leukocyte Mac-1 and viral-infected endothelial cell gC. Although

Table 1. Factor X synthetic peptides. The experimental procedures for the isolation, characterization, and ^{125}I-labeling of factor X have been described (*4*). The human monocytic cell line THP-1 (American Tissue Culture Collection, Rockville, Maryland) was maintained in RPMI 1640 (Irvine Scientific, Santa Ana, California) plus 10% fetal calf serum (Irvine), 25 mM Hepes, 1 mM L-glutamine (Irvine), gentamycin (100 μg/ml) (Geramycin; Schering, Kenilworth, New Jersey), and 10 μM 2-mercaptoethanol (Eastman Kodak). Factor X synthetic peptides were purified by high-pressure liquid chromatography on C-18 columns, dissolved in water at neutral pH at 5 to 10 mM stock concentration, and tested in a quantitative receptor-ligand interaction (*16*). For each synthetic peptide is given the position in the factor X molecule according to Fung *et al.* (*17*), the amino acid sequence in single-letter code, and the corresponding domain in factor X (*6*). Data are shown as a percent of inhibition of specific ^{125}I–factor X binding to THP-1 cells in a representative experiment. EGF-like peptide 82 to 89 (G)ELFTRKL(G), and heavy chain peptides 305 to 320 (Y)ERDAWAESTLMTQKTGI, and 332 to 344 RQSTRLKMLEVPY(K) did not produce titratable dose-dependent inhibition of ^{125}I–factor X binding to THP-1 cells nor inhibition of monocyte adhesion to HSV-infected endothelium and were not further investigated. The apparent increase in ^{125}I–factor X binding in the presence of heavy chain peptides 253 to 270 TEQE*GGEAVHEVEWIK, 384 to 394 VTRFKDTYFVT, and 404 to 414 ARKGKYGIYTK was not observed for lower peptide doses (0.1 mM), thus presumably reflecting self-aggregation of the ligand. Underlined, the tripeptide sequence RGD (*3*). In parentheses, residues added to the natural sequence. *, deletions.

Position	Sequence	Domain	Inhibition (%)
162–187	PYDAADLDPTENPFDLLDFNQTQPER	Activation peptide	38
163–170	YDAADLDP	Activation peptide	27
163–183	YDAADLDPTENPFDLLDFNQT	Activation peptide	25
174–183	PFDLLDFNQT	Activation peptide	0
174–201	PFDLLDFNQTQPERGDNNLTRIVGGQEC	Activation peptide	0
56–60	(G)QNQGK(G)	EGF-like	0
62–69	(G)KDGLGEYT(G)	EGF-like	13
73–80	(G)LEGFEGKN(G)	EGF-like	5
82–89	(G)ELFTRKL(G)	EGF-like	35
130–139	YPCGKQTLER	Light chain	6
211–222	LLINEENE(G)G	Heavy chain	12
237–262	CLYQAKRFKVRVGDRNTEQEEGGEAV	Heavy chain	70
238–254	LYQAKRF***EGDRNTEQEEGG	Heavy chain	0
253–270	TEQE*GGEAVHEVEWIK	Heavy chain	+39
267–279	WIKHNRFTKETYDFDI	Heavy chain	12
284–303	AVLRLKTPITFRMNVAPACL	Heavy chain	7
305–320	(Y)ERDWAESTLMTQKTGI	Heavy chain	35
325–338	(Y)GRTHEKGRQSTRLK	Heavy chain	24
332–344	RQSTRLKMLEVPY(K)	Heavy chain	45
363–375	FCAGYDTKQEDAC	Heavy chain	78
384–394	VTRFKDTYFVT	Heavy chain	+26
404–414	ARKGKYGIYTK	Heavy chain	+11
417–431	AFLWKIDRSMKTRGL	Heavy chain	75

Table 2. Effects of factor X synthetic peptides on monocyte procoagulant activity and monocyte adhesion to HSV-infected endothelium. Monocyte procoagulant activity was assayed as factor Xa generation (*4*). Serum-free suspensions of THP-1 cells at 1.5×10^7 per milliliter were mixed with 100 μM ADP (Sigma), 2.5 mM $CaCl_2$, and 15.1 nM factor X for 30 min at room temperature. Factor Xa formed under these conditions was measured in a sensitive clotting assay using factor VII– and factor X–deficient plasma (Sigma), and quantitated by means of a standard curve constructed with serial concentrations of factor Xa from 10 to 300 ng/ml. Monocyte adhesion to control or HSV-infected endothelium was quantitated after 2 hours incubation at 4°C by use of ^{51}Cr-labeled cells as described (*5*). Under both experimental conditions, synthetic peptides were at 500 μM final concentration. Factor Xa generation by stimulated monocyte THP-1 suspensions in the presence of control scrambled peptides was 35.7 ± 2.7 and 177.1 ± 10 ng/ml, after 5- and 20-min incubation, respectively. In the presence of each of the three inhibitory peptides individually factor Xa formation was reduced to 14.4 ± 2.1 (5 min) and 31.8 ± 11.5 ng/ml (20 min) (peptide 366 to 373 GYDTKQEDG); 16.2 ± 5.7 (5 min) and 44.3 ± 17 ng/ml (20 min) (peptide 422 to 430, IDRSMKTRG); 12 ± 0.6 (5 min) and 30.6 ± 10.5 ng/ml (20 min) (peptide 238 to 246, GLYQAKRFKVG). Control monocyte adhesion to noninfected or HSV-infected endothelium was 1.54 ± 0.29, and 3.4 ± 0.5 monocytes bound (MB) per endothelial cell (EC), respectively. Monocyte adhesion to HSV-infected endothelium in the presence of control scrambled versions of each peptide was 3.3 ± 0.4 (peptide 1, 366 to 373), 3.2 ± 0.65 (peptide 2, 422 to 430), and 3.8 ± 0.3 (peptide 3, 238 to 246) MB per EC, respectively. Data for both monocyte procoagulant activity and monocyte adhesion to HSV-infected endothelium are presented as mean ± SEM of three independent experiments.

Peptide	Factor Xa (ng/ml)	EC adhesion (MB per EC)
Control	346.8 ± 27	3.3 ± 0.4
GYDTKQEDG	95.8 ± 21.8	1.48 ± 0.16
IDRSMKTRG	112.0 ± 36	1.54 ± 0.17
GLYQAKRFKVG	118.4 ± 67	1.46 ± 0.26

unrelated in primary sequence and overall architecture, the HSV-encoded gC (*10*), and the leukocyte integrin Mac-1 (*11*), have evolved a similar ligand recognition repertoire, both including complement proteins of the C3b cascade and factor X (*3, 12*), presumably through convergent evolution. Third, these studies directly link the ligand recognition of a broadly distributed leukocyte integrin such as Mac-1 (*3*) to established mechanisms of vascular injury. These are well exemplified by the recognized atherosclerotic risk associated with HSV infection of endothelial cells (*13*).

The synthetic peptidyl analogs of the ligand loops described here have the capacity to interrupt generation of thrombin on monocytes and HSV-infected endothelium, thereby preventing the pleiotropic consequences that include chemotaxis and mitogenesis (*14*), platelet and leukocyte adhesion to endothelium (*15*), and monocyte deposition of insoluble fibrin (*4*). Moreover, only one of these peptides minimally interferes with the mechanism of factor X activation mediated through the classic extrinsic pathways (*8*). Such specificity suggests that antagonists based on peptidyl analogs or more advanced derivatives may beneficially intervene in related forms of vascular injury without interfering with physiologic hemostatic mechanisms or leukocyte adhesion reactions.

REFERENCES AND NOTES

1. J. Niemetz and K. Fani, *Nature New Biol.* **232**, 247 (1971).
2. D. M. Stern, P. P. Nawroth, W. Kisiel, G. Vehar, C. T. Esmon, *J. Biol. Chem.* **260**, 6717 (1985); G. J. Broze, Jr., *J. Clin. Invest.* **70**, 526 (1982); P. B. Tracy, J. M. Peterson, M. E. Nesheim, F. C. McDuffie, K. G. Mann, *J. Biol. Chem.* **254**, 10354 (1979); I. Maruyama, H. H. Salem, P. W. Majerus, *J. Clin. Invest.* **74**, 224 (1984).
3. E. Ruoslahti, *J. Clin. Invest.* **87**, 1 (1991); M. A. Arnaout, *Blood* **75**, 1037 (1990); T. S. Springer, *Nature* **346**, 425 (1990).
4. D. C. Altieri and T. S. Edgington, *J. Biol. Chem.* **263**, 7007 (1988); D. C. Altieri, J. H. Morrissey, T. S. Edgington, *Proc. Natl. Acad. Sci. U.S.A.* **85**, 7462 (1988).
5. O. R. Etingin, R. L. Silverstein, H. M. Friedman, D. P. Hajjar, *Cell* **61**, 657 (1990).
6. The single-letter abbreviations for the amino acid residues are as follows: A, Ala; C, Cys; D, Asp; E, Glu; F, Phe; G, Gly; H, His; I, Ile; K, Lys; L, Leu; M, Met; N, Asn; P, Pro; Q, Gln; R, Arg; S, Ser; T, Thr; V, Val; W, Trp; and Y, Tyr.
7. Sequence-specific antibodies were raised in rabbits against selected synthetic peptides coupled in equal molar ratio to keyhole limpet hemocyanin. Sera reacting with immobilized factor X in solid phase radioimmunoassay were further purified by affinity chromatography over a 25-ml column of factor X coupled to agarose (2 mg/ml). The immunoglobulin G fraction from each antiserum was obtained by gel filtration on a Protein A–agarose column. In inhibition experiments, increasing concentrations of the various sequence-specific antibodies were preincubated with 15 nM ^{125}I–factor X for 30 min at 22°C before addition to suspensions of N-fMLP–stimulated monocyte THP-1 cells. Fifty per cent inhibition of ^{125}I–factor X binding was achieved with 10 μg/ml of each antibody to the three inhibitory peptides. Under the same experimental conditions, a sequence-specific antibody to the activation peptide of factor X (*21* to *41*) was ineffective.
8. A. Chattopadhyay and D. S. Fair, *J. Biol. Chem.* **264**, 11035 (1989).
9. S. C. T. Lam *et al.*, *ibid.* **262**, 947 (1987); S. A. Santoro and W. Lawing, *Cell* **48**, 867 (1987).
10. R. J. Frink, R. Eisenberg, G. Cohen, E. K. Wagner, *J. Virol.* **45**, 634 (1983).
11. T. K. Kishimoto, K. O'Connor, A. Lee, T. M. Roberts, T. A. Springer, *Cell* **48**, 681 (1987); A. L. Corbi, T. K. Kishimoto, L. Miller, T. A. Springer, *J. Biol. Chem.* **263**, 12403 (1988); M. A. Arnaout, E. Remold-O'Donnel, M. W. Pierce, P. Harris, D. G. Tenen, *Proc. Natl. Acad. Sci. U.S.A.* **85**, 2776 (1988).
12. H. M. Friedman, G. H. Cohen, R. J. Eisenberg, C. A. Seidel, D. B. Cines, *Nature* **309**, 633 (1984).
13. E. P. Benditt, T. Barrett, J. K. McDougall, *Proc. Natl. Acad. Sci. U.S.A.* **80**, 6386 (1983); M. R. Visser *et al.*, *ibid.* **85**, 8227 (1988); D. P. Hajjar, K. B. Pomerantz, D. J. Falcone, B. B. Weksler, A. J. Grant, *J. Clin. Invest.* **80**, 1317 (1987).
14. K. C. Glen and D. D. Cunningham, *Nature* **278**, 711 (1979); R. Bar-Shavit, A. Kahn, G. D. Wilner, *Science* **220**, 728 (1983).
15. S. R. Hanson and L. A. Harker, *Proc. Natl. Acad. Sci. U.S.A.* **85**, 3184 (1988); G. A. Zimmerman, T. M. McIntyre, S. M. Prescott, *J. Clin. Invest.* **76**, 2235 (1985).
16. For peptide competition experiments, 0.2-ml aliquots of THP-1 cells resuspended at 1.5×10^7 per milliliter in serum-free RPMI 1640 were stimulated with 10 μM N-fMLP (Sigma) in the presence of 2.5 mM $CaCl_2$, and simultaneously mixed with 15 nM ^{125}I–factor X and 0.5 mM doses of the various factor X synthetic peptides for 20 min at 22°C. The reaction was terminated by centrifugation through mixture of silicone oil (Dow Corning, New Bedford, MA) and nonspecific binding calculated in the presence of a 100-fold molar excess of unlabeled factor X was subtracted from the total to calculate net specific binding. ^{125}I–factor X specifically bound to N-fMLP–stimulated THP-1 cells in the absence of competing peptides was 57,000 ± 8,000 molecules per cell ($n = 10$).
17. M. R. Fung, C. W. Hay, R. T. A. MacGillivray, *Proc. Natl. Acad. Sci. U.S.A.* **82**, 3591 (1985).
18. J. Greer, *Proteins Struct. Funct. Genet.* **7**, 317 (1990).
19. Trypsinogen structure (2TGP) from Marquart *et al.* (*22*) as contained in the Brookhaven National Laboratory, F. C. Bernstein *et al.* [*J. Mol. Biol.* **112**, 535 (1977)], and E. E. Abola *et al.* [*Protein Data Bank*, in *Crystallographic Databases–Information Content, Software Systems, Scientific Applications*, F. H. Allen, G. Bergenhoff, R. Sievers, Eds. (Data Commission of the International Union of Crystallography, Bonn, Cambridge, and Chester, 1987), p. 107].
20. Trypsin (2PTC) from (*22*). Chymotrypsin (5CHA) from R. A. Blevins and A. Tulinsky [*J. Biol. Chem.* **260**, 4264 (1985)]. Elastase (1EST) from L. Sawyer *et al.* [*J. Mol. Biol.* **118**, 137 (1978)]. Kallikrein (2PKA) from W. Bode *et al.* [*ibid.* **164**, 237 (1983)].
21. T. K. Brunck, personal communication.
22. M. Marquart *et al.*, *Acta Crystallogr.* B39, 480 (1983).

23. Supported by National Institutes of Health grants R01 HL 43773, P01 HL 16411, HL 46408, HL 18828, and HL 45343. This is manuscript 6818-IMM from the Department of Immunology. D. S. Fair died 12 May 1990.

25 June 1991; accepted 11 September 1991

Epidermolysis Bullosa Simplex: Evidence in Two Families for Keratin Gene Abnormalities

J. M. BONIFAS, A. L. ROTHMAN, E. H. EPSTEIN, JR.*

Epidermolysis bullosa simplex (EBS) is characterized by skin blistering due to basal keratinocyte fragility. In one family studied, inheritance of EBS is linked to the gene encoding keratin 14, and a thymine to cytosine mutation in exon 6 of keratin 14 has introduced a proline in the middle of an alpha-helical region. In a second family, inheritance of EBS is linked to loci that map near the keratin 5 gene. These data indicate that abnormalities of either of the components of the keratin intermediate filament heterodipolymer can impair the mechanical stability of these epithelial cells.

EPIDERMOLYSIS BULLOSA SIMPLEX IS an unusual hereditary disorder in which patients develop blisters after relatively mild mechanical trauma. Cleavage is through the basal cells, unlike the more superficial cleavage that produces friction blisters in normal people. Those with the commonest forms of EBS have blisters predominantly acrally (EBS–Weber-Cockayne or EBS-WC) or in a more generalized distribution (EBS-Koebner or EBS-K). Skin fragility is temperature sensitive—it is worse in the summer, and preventive measures are confined to cooling the skin and avoiding trauma. Although the blisters heal relatively quickly and without scarring, blistering may be so painful as to be medically disabling (*1*).

Several years ago we were struck by similarities between EBS and heritable erythrocyte disorders such as pyropoikilocytosis, elliptocytosis, and spherocytosis. These similarities include autosomal dominant inheritance and temperature-sensitive cellular fragility. These red blood cell disorders result from molecular abnormalities of the cytoskeleton, which is limited in the mature erythrocyte to a submembranous position. Although keratinocytes do contain homologs of proteins of the erythrocyte membrane skeleton (*2*), their predominant cytoskeletal components are the tonofilaments—intermediate filaments composed of keratin

Department of Dermatology, San Francisco General Hospital, University of California, San Francisco, CA 94110.

*To whom correspondence should be addressed.